Cognitive Phenotypes in Parkinson's Disease Differ in Terms of Brain-Network Organization and Connectivity

◆ Human Brain Mapping 38:1604–1621 (2017) ◆

Cognitive Phenotypes in Parkinson's Disease Differ in Terms of Brain-Network Organization and Connectivity

Renaud Lopes,[1,2,3] Christine Delmaire,[1,2,3] Luc Defebvre,[1,2,4] Anja J. Moonen,[5] Annelien A. Duits,[5] Paul Hofman,[6] Albert F.G. Leentjens,[5] and Kathy Dujardin[1,2,4]*

[1]Univ. Lille, U1171 - Degenerative & vascular cognitive disorders, Lille, France
[2]Inserm, U1171, Lille, France
[3]Neuroimaging Department, CHU Lille, Lille, France
[4]Neurology and Movement Disorders Department, CHU Lille, Lille, France
[5]Department of Psychiatry, Maastricht University Medical Centre, Maastricht, the Netherlands
[6]Department of Radiology, Maastricht University Medical Centre, Maastricht, the Netherlands

Abstract: Cognitive deficits are common in Parkinson's disease and we suspect that dysfunctions of connected brain regions can be the source of these deficits. The aim of the present study was to investigate changes in whole-brain intrinsic functional connectivity according to differences in cognitive profiles in Parkinson's disease. 119 participants were enrolled and divided into four groups according to their cognitive phenotypes (determined by a cluster analysis): (i) 31 cognitively intact patients (*G*1), (ii) 31 patients with only slight mental slowing (*G*2), (iii) 43 patients with mild to moderate deficits mainly in executive functions (*G*3), (iv) 14 patients with severe deficits in all cognitive domains (*G*4–5). Rs-fMRI whole-brain connectivity was examined by two complementary approaches: graph theory for studying network functional organization and network-based statistics (NBS) for exploring functional connectivity amongst brain regions. After adjustment for age, duration of formal education and center of acquisition, there were significant group differences for all functional organization indexes: functional organization decreased ($G1 > G2 > G3 > G4$-5) as cognitive impairment worsened. Between-group differences in functional connectivity (NBS corrected, $P < 0.01$) mainly concerned the ventral prefrontal, parietal, temporal and occipital cortices as well as the basal ganglia. In Parkinson's disease, brain network organization is progressively disrupted as cognitive impairment worsens, with an increasing number of altered connections between brain regions. We observed reduced connectivity in highly

Additional Supporting Information may be found in the online version of this article.

The sponsor was not involved in the study design or in data interpretation, writing of the report or decision to submit the article for publication.
Contract grant sponsor: Michael J. Fox Foundation for Parkinson's research

*Correspondence to: Kathy Dujardin, Neurologie et Pathologie du Mouvement, Neurologie A, Hôpital Salengro, Centre Hospitalier Universitaire, F-59037 Lille cedex, France. E-mail: kathy.dujardin@univ-lille2.fr

Received for publication 1 June 2016; Revised 28 October 2016; Accepted 8 November 2016.
DOI: 10.1002/hbm.23474
Published online 17 November 2016 in Wiley Online Library (wileyonlinelibrary.com).

associative areas, even in patients with only slight mental slowing. The association of slowed mental processing with loss of connectivity between highly associative areas could be an early marker of cognitive impairment in Parkinson's disease and may contribute to the detection of prodromal forms of Parkinson's disease dementia. *Hum Brain Mapp 38:1604–1621, 2017*.

Key words: cognition; dementia; fMRI; resting state connectivity

INTRODUCTION

Parkinson's disease is a neurodegenerative disease affecting more than 1% of the population over the age of 60 [de Lau and Breteler, 2006]. Besides the hallmark motor symptoms (rest tremor, hypokinesia, rigidity and postural instability), cognitive deficits are common in Parkinson's disease. In untreated, newly diagnosed patients, their prevalence is estimated around 20 to 30% [Barone et al., 2011; Elgh et al., 2009; Muslimovic et al., 2005]. On average, 26.7% (range: 18.9%–38.2%) meet the criteria for mild cognitive impairment [Litvan et al., 2011] whose prevalence increases with age, disease duration and severity of Parkinson's disease. In cross-sectional studies, 30–40% of patients meet criteria for dementia [Emre, 2003; Emre et al., 2007] and the cumulative incidence may be as high as 80–90% [Aarsland et al., 2005; Buter et al., 2008; Hughes et al., 2000]. There is a substantial heterogeneity in the clinical presentation of cognitive deficits in Parkinson's disease [Tröster, 2011] but also in their progression [Halliday and McCann, 2010; Reid et al., 2011]. Most studies on cognitive phenotypes in Parkinson's disease have used predefined categories, yet in a previous study, we used a data-driven approach in a large group of patients ($n = 557$) who underwent a standardized neuropsychological assessment and we identified five cognitive profiles on a spectrum going from cognitively intact patients with high level of performance to patients with severe deficits in all cognitive domains [Dujardin et al., 2013]. We recently confirmed these results in an independent cohort of 156 patients [Dujardin et al., 2015]. The finding of a spectrum of severity of cognitive impairment in Parkinson's disease suggests that the identified cognitive phenotypes probably not emerge from focused atrophy or dysfunction of specific brain regions but are more likely related to alterations in information processing by different brain regions involved in functional networks. In the present study, our aim was to determine whether these cognitive phenotypes were associated with specific changes in markers of brain functional organization.

Resting state functional magnetic resonance imaging (rs-fMRI) has been shown to be particularly relevant to investigate large-scale brain network organization [Biswal et al., 1995; Fox and Raichle, 2007]. This non-invasive method allows investigation of brain changes associated with a disease by focusing on low-frequency spontaneous fluctuations in the blood-oxygenation-level-dependent (BOLD) signal that occur at rest [Prodoehl et al., 2014]. Recently, the combination of rs-fMRI and graph-based network analysis revealed the topological organization of human whole-brain functional networks, such as, network efficiency and modularity [for reviews, see (Bullmore and Sporns, 2009)]. rs-fMRI studies in PD first explored functional connectivity of the motor network [Helmich et al., 2010; Wu et al., 2009; Wu et al., 2011] and, more recently, changes in brain connectivity associated with cognitive disorders. The latter studies aimed to investigate changes in the three core neurocognitive networks considered as playing a critical role in the pathophysiology of cognitive disorders: the default-mode network (DMN), the salience network and the central executive network [Bressler and Menon, 2010]. Several studies found that decreased functional connectivity within the DMN was associated with cognitive impairment in Parkinson's disease [Olde Dubbelink et al., 2014; Rektorova et al., 2012; Tessitore et al., 2012]. Baggio et al. [Baggio et al., 2014] used rs-fMRI and graph-theory-based network analysis to explore global and local brain connectivity in 84 Parkinson's disease patients of which 35% had a mild cognitive impairment (PD-MCI), and 38 matched healthy controls. Decreases in widespread long-range connectivity were observed in the Parkinson's disease group as a whole but were greater in the PD-MCI

Abbreviations

AUC	Area under the curve
BOLD	Blood-oxygen-level dependent
C_p	Clustering coefficient
DMN	Default mode network
E_g	Global efficiency
E_{loc}	Local efficiency
EPI	Echo planar imaging
FDR	False discovery rate
Lp	Mean path length
MNI	Montreal neurological institute
MDS-UPDRS	Movement Disorders Society - Unified Parkinson Disease Rating Scale
NBS	Network-based statistitics
PD-MCI	Parkinson's disease with mild cognitive impairment
ROI	Region of interest
Rs-fMRI	Resting-state functional magnetic resonance imaging
SD	Standard deviation
TE	Echo time
TR	Repetition time

subgroup in which all the connections between the major cortical and subcortical areas were concerned. Increases in local connectivity were also observed, which were associated with deficits in visuospatial functions and memory. These authors also investigated whether the three groups differed in terms of connectivity within the three core neurocognitive networks [Baggio et al., 2015b] and found reduced connectivity between right fronto-insular regions and the dorsal attention network in the PD-MCI subgroup. This reduced connectivity was associated with decreased performance in attention and executive functions. They also observed an increased connectivity between posterior cortical regions and the DMN, associated with deficits in visuospatial functions.

In the present study, we hypothesized that the spectrum of cognitive impairment we observed in our previous studies results from changes in brain functional organization. We used two approaches for assessing these changes in whole-brain functional connectivity. Firstly, network topology was investigated by graph theory to quantify alterations in segregation, integration and degree distribution of the functional network. Secondly, functional connectivity amongst 164 brain regions was explored using network-based statistics to quantify focal alterations in the network [Zalesky et al., 2010]. Our main hypothesis was that cognitive profiles in Parkinson's disease differ in terms of functional network organization and patterns of functional connectivity between the cortical regions. More specifically, we expected that progression of cognitive decline would be associated with decreased functional segregation and integration of the network (markers of the organization of the brain regions connections). We also hypothesized that the different cognitive profiles will differ in terms of patterns of functional connectivity between brain regions. Finally, patterns of connectivity were correlated with performance on the neuropsychological tests in order to determine whether specific changes in the topological organization of the brain are markers of a cognitive phenotype.

MATERIALS AND METHODS

Participants and Assessment

The present study follows a cross-sectional study that aimed to identify cognitive phenotypes in Parkinson's disease. One hundred fifty-six Parkinson's disease patients participated in the study. All patients met the United Kingdom Brain Bank criteria for idiopathic Parkinson's disease [Gibb and Lees, 1988] and none was suffering from a neurological disease other than Parkinson's disease. Patients with moderate and severe dementia (defined as a score >1 on the Clinical Dementia Rating [Morris, 1993] and according to the Movement Disorders criteria [Emre et al., 2007]) and those older than 80 years were excluded. They were recruited among the outpatients of two independent European movement disorder centers, in Lille, France and Maastricht, the Netherlands. All participants gave their informed consent to participation in the study, which had been approved by the local institutional review boards (CPP Nord-Ouest IV, 2012-A 01317-36, ClinicalTrials.gov Identifier: NCT01792843).

All patients underwent a comprehensive neuropsychological assessment including tests for global cognition and standardized tests representing five cognitive domains: (1) attention and working memory (Digit span forward and backward [Wechsler, 1986], Symbol Digit Modalities Test [Smith, 1982]) (2) executive functions (Trail Making Test B/A ratio [Reitan, 1992], the interference index and the number of errors in the interference condition of a 50-item version of the Stroop word color test and a 1-minute phonemic word generation task performed in single and alternating conditions) (3) verbal episodic memory (Hopkins verbal learning test [Brandt and Benedict, 2001]), (4) language (the 15-item short form of the Boston naming test [Graves et al., 2004] and animal names generation task in 1 minute), (5) visuospatial functions (the short version of the judgment of line orientation test [Benton et al., 1978]). A cluster analysis (based on the k-means method) performed on the neuropsychological variables identified five phenotypes that were used for separating the participants according to their cognitive status: (1) cognitively intact patients with high level of performance in all cognitive domains, (2) cognitively intact patients with only slight mental slowing, (3) patients with mild to moderate deficits in executive functions, (4) patients with severe deficits in all cognitive domains, particularly executive functions, (5) patients with severe deficits in all cognitive domains, particularly working memory and recall in verbal episodic memory (for details, see [Dujardin et al., 2015]).

Detailed demographic and disease related variables were recorded likewise. All the patients' medications were checked and doses of antiparkinsonian medication were converted to levodopa equivalent daily dose according to the algorithm by Tomlinson et al. [2010]. Severity of motor symptoms was assessed by the score on the Movement Disorders Society—Unified Parkinson Disease Rating Scale (MDS-UPDRS)—part III [Goetz et al., 2008] and disease stage by the Hoehn & Yahr score [Hoehn and Yahr, 2001]. The severity of depression, apathy and anxiety symptoms was quantified with the 17-item Hamilton Depression Rating Scale [Hamilton, 1960], the Lille Apathy Rating Scale [Sockeel et al., 2006] and the Parkinson Anxiety Rating Scale [Leentjens et al., 2014], respectively. The presence and severity of hallucinations was assessed by the score on the item 1.2 of the MDS-UPDRS.

All patients were assessed after having received their usual anti-parkinsonian medication and were in their "best on" state.

MRI Acquisition

Patients were scanned at two sites (Maastricht and Lille) using the same 3T MRI scanner (Philips Achieva) with

identical software versions and MR sequences. High-resolution 3D T1-weighted images were acquired with a magnetization-prepared gradient echo sequence (voxel size: 0.750 × 0.727 × 0.727 mm^3; TR: 10.4 ms; TE: 4.76 ms; matrix size: 214 × 352 × 352 voxels). Resting-state functional imaging (rs-fMRI) was performed with a T2*-weighted EPI sequence lasting 10 min (voxel size: 3 × 3 × 3 mm^3; TR: 2400 ms; TE: 30 ms; matrix size: 64 × 64 × 40 voxels; flip angle: 90°). Patients were required to remain quiet, stay awake and close their eyes.

One hundred thirty-four of the participants had an MRI scan. For the quality control of the data, all images were visually inspected by an investigator (CD) and rs-fMRI images with largely incomplete brain coverage, high movement peaks, ghosting or large motion artefacts were excluded. The displacements were computed using the six parameters (three rotations and three translations) from the rigid registration algorithm (for details, see section "Functional MRI pre-processing"). Rotational framewise displacements were adjusted to be expressed as a millimeter displacement for a typical distance from the center of 50 mm (Power et al., 2012). The sum of the absolute value of the six displacement measures were calculated for each frame and scrubbing frames were defined as those for which the value was greater than two standard deviations from the mean displacement. Subjects whose scrubbing frames represented more than 15% of all the frames were excluded. Five patients were excluded from the study because of brain lesions (thalamic lacunar infarctions, left prefrontal, bilateral orbito-frontal and two cases of temporal ischemic lesions), four patients with poor quality of T1 image and six patients with motion artefacts in rs-fMRI data. As a result, one hundred nineteen participants were included in the present study and divided into four groups according to the cognitive phenotypes (due to the low number of subjects, participants of the two groups with severe cognitive deficits were merged into one group): (1) 31 cognitively intact patients with high level of performance in all cognitive domains—" *G*1," (2) 31 cognitively intact patients with only slight mental slowing—" *G*2," (3) 43 patients with mild to moderate deficits, mainly in executive functions—" *G*3," (4) 14 patients with severe deficits in all cognitive domains—" *G*4-5."

Functional MRI Pre-Processing

First, pre-processing of fMRI data included the removal of the first three image volumes (to avoid T1 equilibration effects), rigid-body head motion correction to the first frame of data, and slice-timing correction using the first frame as the reference. Then, the distortion field, inherent to EPI images in the phase encoding direction and responsible for geometric and signal artefacts, was calculated using a pair of spin echo EPI scans with opposite phase encoding directions [Holland et al., 2010]. The FSL toolbox "topup" [Andersson et al., 2003] was used to estimate the distortion field, which was applied to correct all fMRI images.

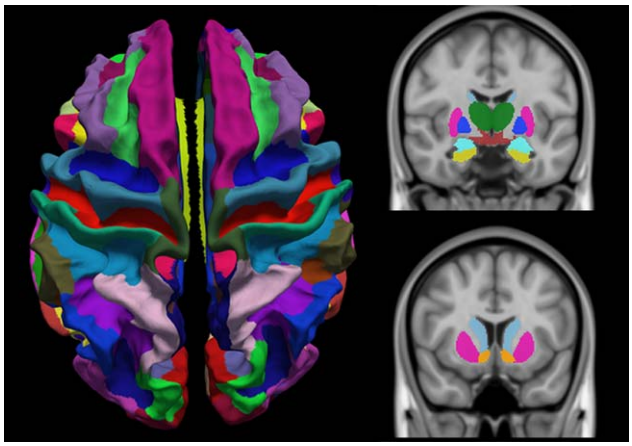

Figure 1.
Brain parcellation in 148 cortical regions based on the Destrieux atlas and 16 subcortical regions. [Color figure can be viewed at wileyonlinelibrary.com]

Brain Parcellation and Registration to Functional MRI

Structural T1-weighted images were processed using the Freesurfer software (http://surfer.nmr.mgh.harvard.edu/). This included the pre-processing steps of non-uniform signal correction, signal and spatial normalizations, skull stripping and brain tissues segmentation [Dale et al., 1999]. Freesurfer software provided parcellation of anatomical regions of cortices (74 for each hemisphere) based on the Destrieux atlas and subcortical regions (eight for each hemisphere: nucleus accumbens, amygdala, caudate, hippocampus, pallidum, putamen, thalamus and ventral diencephalon). In total, 164 regions of interest (ROIs) were studied (Fig. 1). ROIs defined in T1 space had to be transformed into fMRI space where all calculations were made. T1 images were registered to the fMRI data using boundary-based registration [Greve and Fischl, 2009]. This method is more accurate than common registration algorithm, such as correlation ratio and normalized mutual information. The first frame of the pre-processed fMRI data was chosen as the template image. The cross-modality registration was achieved by minimizing the misalignment between the cortical grey-white boundaries in the anatomical and fMRI template image through six degrees of freedoms. Finally, ROIs and brain tissues segmentation masks (white matter and cerebrospinal fluid) were resampled to fMRI space. Parcellation and registration were manually checked for errors by visual inspection.

Network Construction

Two additional processing steps on fMRI data were added before the computation of the functional connectivity. Firstly, the physiological signal fluctuations were removed by a brain tissue-based correction approach called CompCor [Behzadi et al., 2007]. This method

required white matter and cerebrospinal fluid masks extracted from the T1 image in the previous section. After a first regression to remove linear/quadratic trends (to account for scanner drift) and six motion parameters, the top five principal components from both masks were regressed out from each BOLD signal. Secondly, residual fMRI data were low-pass filtered, such that only frequencies below 0.1 Hz were selected.

A network or graph G = (V,E) is composed of nodes V and edges E between nodes. Herein, the functional network was obtained from the defined and registered ROIs and BOLD signal. The nodes represented the one hundred sixty-four ROIs and the edges represented the linear correlation between the mean BOLD time-courses in two given ROIs. For each participant, a 164x164 symmetric weighted network was constructed. Finally, as age, formal education duration and participating centre differed across groups, the weighted network was corrected for all three by regressing out these factors of each participant from weighted edges.

Statistical Analyses

The network analyses were performed at two scales: network scale and edges scale. At the network scale, functional organization indexes of brain networks were computed using GRETNA toolbox (https://www.nitrc.org/projects/gretna/): the functional segregation, the functional integration and the degree distribution. At the edge scale, the alterations in functional connectivity were investigated using network-based statistics.

Network Topology Analysis

Functional segregation and integration (graph theory measures)

The corrected weighted network was thresholded at different levels of sparsities ranging from 10% to 40% using increments of 1%, in keeping the highest weighted edges. At each threshold, global network metrics were calculated: the clustering coefficient C_p, the mean path length L_p, the global efficiency E_g and the local efficiency E_{loc}. The area under the curve (AUC) for each network metric was calculated to provide a summarized scalar for topological organization of brain networks independent of a single threshold selection [Achard et al., 2006] . The metrics' definitions are briefly described below.

The clustering coefficient C_p of G quantifies the extent of local clustering or cliquishness of a network [Watts and Strogatz, 1998]. It is expressed as follows [Onnela et al., 2005]:

$$C_p(G) = \underset{i \in node}{mean} \frac{2}{k_i(k_i-1)} \sum_{j,k} \left(\overline{w_{ij}}\ \overline{w_{jk}}\ \overline{w_{ki}}\right)^{1/3} \quad (2)$$

where k_i is the degree of node i ($\sum_{j \neq i \in G} w_{i,j} > 0$), and $\overline{w}$ is the weighted value of the edge, which is scaled by the mean of all weights to control each participant's cost at the same level.

The mean path length L_p of G quantifies the ability for information to be propagated in parallel. It is expressed as follows:

$$L_p(G) = \frac{1}{N(N-1)} \sum_{i \neq j \in G} L_{ij} \quad (3)$$

where L_{ij} is the shortest path length between any pair of nodes i and j and is defined as the sum of the edge weight w_{ij} along this path.

The E_g of G quantifies the global efficiency of the parallel information transfer in the network. It is expressed as follows:

$$E_g(G) = \frac{1}{N(N-1)} \sum_{i \neq j \in G} \frac{1}{L_{ij}} \quad (4)$$

The E_{loc} of G quantifies the fault tolerance of a network, showing how efficient the communication is among the first neighbours of node i when it is removed. It is expressed as follows:

$$E_{loc}(G) = \frac{1}{N(N-1)} \sum_{i \neq j \in G} E_g(G_i) \quad (5)$$

Where G_i denotes the subgraph composed of the nearest neighbours of node i.

Between-group differences in AUC values of network metrics were investigated in a one-way ANOVA after the normality of the data distribution had been checked in a Kolmogorov-Smirnov test. Levene's test showed non-homogeneity of variances within groups, so Welch ANOVA using SPSS 20.0 software (SPSS Inc., Chicago, IL, USA) was performed on data. Metrics showing main effect of group difference in ANOVA model were further evaluated by post-hoc tests (Games-Howell test). A significance threshold of $P < 0.01$ was applied to each test and the FDR was used to correct for multiple comparisons.

Degree distribution

The degree distribution $P(k)$ of a graph is the fraction of nodes with degree k, and can be used to assay the hierarchy of hubs in the network. The analysis was performed on the sparsest binary network (10%) to eliminate the weaker noisy connections [Achard et al., 2006]. Brain networks may be fitted for three candidate models based on the frequency distribution of their node degrees:

$$\text{Exponential:}\quad P(K) = e^{-\beta K} \quad (6)$$

$$\text{Power-law:}\quad P(K) = K^{-\alpha} \quad (7)$$

$$\text{Exponentially truncated power-law:}\quad P(K) = K^{\alpha-1} e^{K/\beta} \quad (8)$$

Where K denotes degree, α the power law exponent and the β exponential cutoff.

TABLE I. Demographic and clinical features (mean (SD), unless otherwise indicated) of the four patient subgroups

N = 119	Group 1	Group 2	Group 3	Group 4	*P* value
n (%)	31 (26.05)	31 (26.05)	43 (36.13)	14 (11.76)	
Center (Lille/Maastricht)	8/23	16/15	31/12	10/4	0.001
Demographic					
Sex (% male)	67.74	77.42	60.46	71.43	0.482
Age (y)	60.19 (8.37)	64.56 (6.23)	66.65 (7.92)	69.82 (6.09)	<0.001
Formal education (y)	13.45 (3.25)	13.84 (4.41)	11.33 (3.46)	9.36 (2.13)	<0.001
Clinical					
Disease duration (y)	7.52 (5.07)	8.26 (7.48)	8.65 (4.81)	10.36 (6.15)	0.501
MDS_UPDRS3 score	25.19 (10.65)	29.45 (12.29)	27.86 (11.12)	28.71 (17.47)	0.563
Hoehn & Yahr stage	1.87 (0.36)	2.06 (0.44)	2.20 (0.62)	2.21 (8.80)	0.065
Side of onset (% right)	48.39	45.16	44.18	71.42	0.333
Medication					
LEDD (mg/day)	753.00 (696.60)	727.80 (494.54)	862.96 (544.15)	838.80 (275.24)	0.714
Neuropsychiatry					
Hamilton depression rating scale	5.68 (4.39)	5.45 (5.51)	6.28 (4.22)	5.64 (4.24)	0.881
Lille apathy rating scale	−26.68 (6.22)	−26.94 (6.65)	−23.05 (7.00)	−20.93 (7.66)	0.007
Hallucinations (%)	0.00	0.00	34.88	14.29	0.017
Slight hallucinations (*n*)	0	0	10	2	
Mild hallucinations (*n*)	0	0	5	0	
Severe hallucinations (*n*)	0	0	0	0	
Overall cognition					
MMSE/(30)	28.77 (1.12)	28.45 (1.67)	26.98 (2.29)	24.14 (3.55)	<0.001
Mattis DRS (/144)	140.58 (3.22)	140.26 (3.10)	134.56 (5.61)	125.86 (8.48)	<0.001

MDS_UPDRS3 = Movement Disorders Society sponsored revision of the Unified Parkinson's disease Rating Scale-Part III (severity of motor symptoms)[Goetz et al., 2008]; LEDD = Levodopa Equivalent Daily Dose; MMSE = Mini Mental Sate Examination; DRS = dementia rating scale.

These three statistical models were evaluated using Akaike's information criterion. Between-group differences in α and/or β values were assessed by one-way ANOVA and post-hoc tests at a significance threshold of $P < 0.01$, FDR corrected.

Subjects classification based on graph-theory measures

In order to determine if a combination of graph-theory measures could predict the subject groups, we performed a multinomial logistic regression to build classification models (Matlab software). In our model, the predictors were the four network measures and the response was the subject's group. Classification accuracy was evaluated via leave-one-out cross-validation to ensure a relatively unbiased estimate of the generalization power of the classifiers to new subjects. The model was estimated 119 times, each time leaving out a different subject, leading to a cross-validation classification accuracy. The sensitivity and the specificity were calculated from the confusion matrix.

Correlation with cognitive performance

To assess the relationship between the global network indices and cognitive performance, each network metric was correlated with a composite cognitive score. This score was based on the results of a prior study [Dujardin et al., 2015]. Indeed, after the clustering analysis identifying the five cognitive profiles, we carried out a discriminant factorial analysis (for details see, [Dujardin et al., 2015]) revealing that three neuropsychological tests were the most discriminant. It included the number of correct responses at the symbol digit modalities test, the number of errors at the Stroop test and animal fluency in 60 sec. *Z*-scores were calculated for each of these tests and the cognitive score used was the sum of these *Z*-scores. Pearson's correlation coefficients were used and FDR was used to correct for multiple comparisons.

Functional connectivity analysis

To further identify functional connections showing differences in patients groups, the network-based statistics (NBS) approach was used, which is a validated nonparametrical statistical approach for controlling family-wise error in connectome analyses [Zalesky et al., 2010]. NBS was applied to compare patient groups with the following sequence: (1) mean connectivity strengths changes were calculated with permutation tests, (2) network components of connected edges that survived a *P*-value of 0.005 uncorrected were retained, (3) the size of the largest cluster was calculated. To generate an empirical null distribution for evaluating the statistical significance of the cluster sizes, groups were randomly shuffled (20,000 permutations), then the largest cluster size null-distribution was obtained

TABLE II. Performance (mean (SD) at the neuropsychological tests of the four patient subgroups

$N = 119$	Group 1	Group 2	Group 3	Group 4	P value
Attention and working memory					
WAIS-R forward digit (/14)	8.65 (1.62)	7.74 (1.79)	6.63 (2.35)	6.50 (2.62)	<0.001
WAIS-R backward digit (/14)	6.48 (1.52)	6.26 (1.53)	4.72 (1.64)	3.50 (1.58)	<0.001
SDMT: number in 90sec	56.10 (7.11)	43.61 (3.39)	33.26 (6.72)	15.50 (10.43)	<0.001
Executive functions					
Trail Making Test (time B/time A)	2.16 (0.58)	2.46 (0.56)	2.77 (0.75)	2.53 (1.33)	0.010
Stroop: interference index	1.57 (0.41)	1.70 (0.25)	2.09 (0.62)	2.61 (1.22)	<0.001
Stroop: errors	0.58 (1.99)	1.03 (1.25)	4.12 (4.37)	18.93 (14.07)	<0.001
Phonemic fluency (60 sec)	15.32 (5.19)	15.06 (2.64)	10.77 (3.85)	7.64 (3.10)	<0.001
Alternating fluency (60 sec)	14.61 (4.12)	13.29 (3.67)	8.35 (3.39)	6.14 (3.25)	<0.001
Memory					
HVLT Learn1 (/12)	7.29 (1.66)	6.77 (1.52)	5.51 (2.13)	3.43 (1.65)	<0.001
HVLT Learn total (/36)	28.06 (4.12)	26.90 (3.05)	23.33 (4.11)	16.36 (4.89)	<0.001
HVLT delayed recall (/12)	9.84 (1.71)	9.97 (1.78)	8.07 (2.18)	4.71 (2.87)	<0.001
HVLT recognition hits (/12)	11.42 (0.81)	11.58 (0.81)	11.21 (0.94)	9.79 (1.72)	<0.001
HVLT number of intrusions	1.10 (1.56)	1.45 (2.22)	2.33 (3.18)	3.29 (2.23)	0.023
Language					
Boston naming test (/15)	13.77 (1.28)	13.35 (1.78)	11.14 (2.59)	10.64 (2.95)	<0.001
Semantic fluency (animals in 60 sec)	25.58 (4.89)	20.26 (3.60)	15.02 (4.07)	10.64 (5.31)	<0.001
Visuospatial functions					
Judgment of line orientation (/15)	12.90 (2.01)	12.45 (2.67)	10.74 (2.88)	7.14 (3.03)	<0.001

WAIS-R= Wechsler for adults intelligence scale revised; SDMT= Symbol digit modalities test; HVLT = Hopkins verbal learning test.

by repeating steps 1, 2, and 3. Note that while the choice of the NBS threshold value is arbitrary, it can affect only sensitivity and not specificity [Zalesky et al., 2012].

Corrected weighted networks of all groups were entered into a one-way ANOVA in NBS approach ($P < 0.01$ NBS-corrected for multiple comparisons). Post-hoc t-tests were performed to assess between-group differences on the significant network obtained by ANOVA ($P < 0.01$ NBS-corrected for multiple comparisons).

For the visualization purpose, circular graphical representations (called "connectograms") were used to display significant connections in the statistical analyses using Circos software (http://www.circos.ca) [Irimia et al., 2012]. The pair-wise connections were displayed with links colored by connection type: left intra-hemispheric (blue), right intra-hemispheric (green) and inter-hemispheric (red). ROIs were grouped according to broad anatomical divisions (i.e., frontal, insular, cingular limbic, temporal, parietal, occipital, subcortical). The ROIs with a high degree of significant connections ($k > 1$ SD above the mean) were classified as "network hubs" and represented in bold, in accordance with prior work [Baker et al., 2015].

RESULTS

Demographic, Clinical, and Neuropsychological Characteristics

Table I shows the demographical and clinical characteristics of the four patient groups and results of neuropsychological assessment are shown in Table II. As significant between-group differences were observed for age, duration of formal education and number of subjects by participating centre, further analyses were adjusted on these variables. Despite a significant group effect on severity of the apathy symptoms and frequency of hallucinations, these variables were not considered as confounding factors since they have been frequently associated with cognition in Parkinson's disease [Aarsland et al., 2014; Dujardin et al., 2009]. Table I shows that most of the patients with hallucinations only had illusions or not-formed hallucinations (scoring 1 on the item 1.2 of MDS-UPDRS) or formed hallucinations without loss of insight (scoring 2 on the item 1.2 of MDS-UPDRS).

Network Topology

There was a significant difference between groups as determined by one-way ANOVA for global efficiency E_g ($F = 14.10$, $P = 0.000$), clustering coefficient C_p ($F = 8.47$, $P = 0.001$) and local efficiciency E_{loc} ($F = 4.75$, $P = 0.008$) (Fig. 2). A Games-Howell test revealed that E_g was significantly lower for *G*1, *G*2 and *G*3 than *G*4-5. Also, *G*1 showed lower E_g values than *G*2 and *G*3. The C_p values were significantly higher for *G*1 and *G*2 than *G*4-5. Also, *G*1 showed higher Cp values than *G*3. The E_{loc} values were significantly higher for *G*1 and *G*2 than *G*4-5. No statistically significant difference was found between *G*2 and *G*3 for all network metrics.

The best fitting using Akaike's information criterion was obtained with an exponentially truncated power law. Post-hoc tests showed that the power law exponent α was significantly increased but the exponential cutoff β was

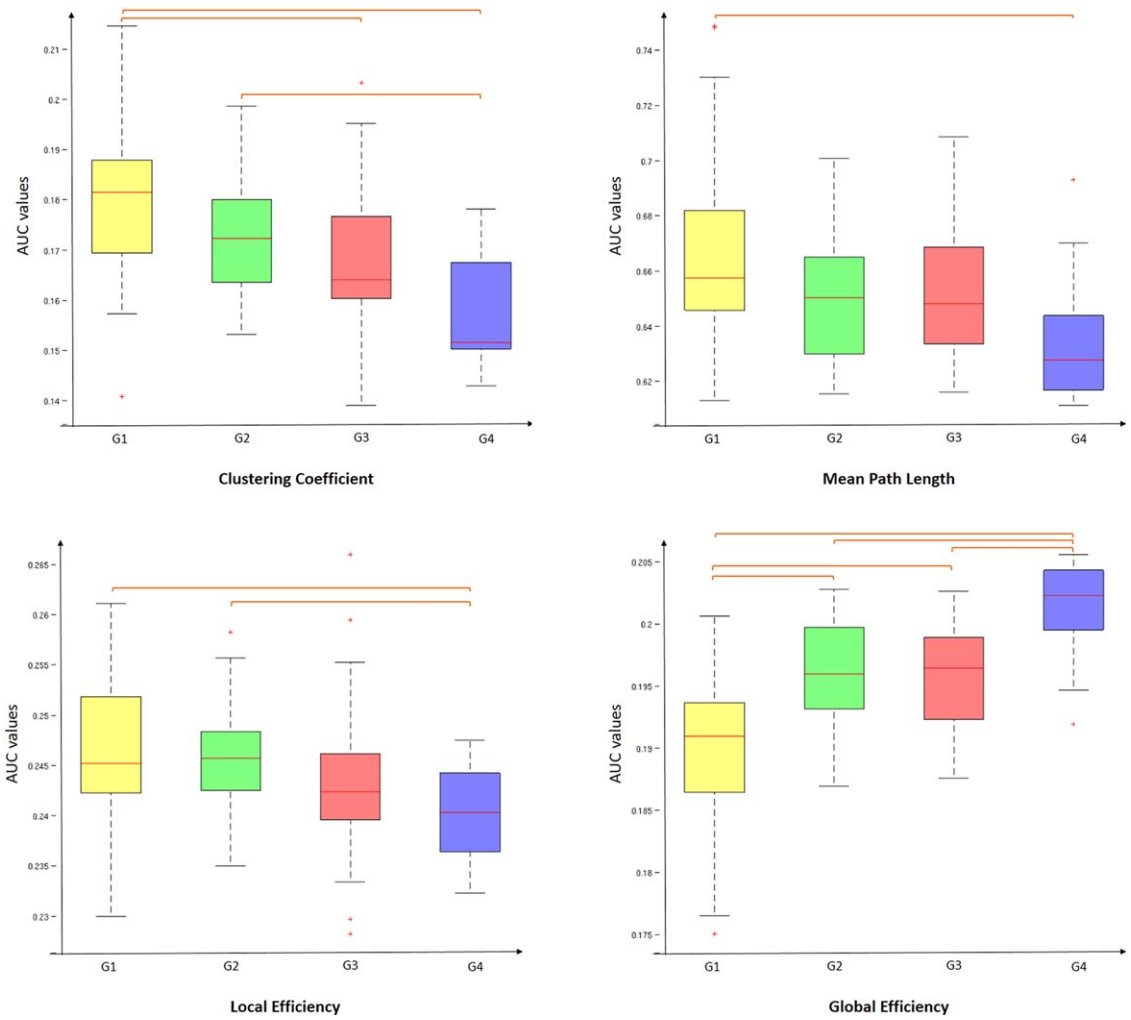

Figure 2.

Boxplot of mean AUC network metrics values for each group. Between-group differences were assessed by one-way ANOVA and post-hoc tests ($P < 0.01$). AUC value corresponds to the area under the curve in plotting the network metric values as a function of the threshold values applied to the connectivity matrix. [Color figure can be viewed at wileyonlinelibrary.com]

significantly reduced in *G*4-5 (Fig. 3). These distribution parameters indicate that the probability of high degree hubs is reduced in *G*4-5.

The leave-one-out cross-validation classification procedure was applied using the four network measures and the performance is summarized in Table III. A classification accuracy of 75% was obtained for all subjects. However, the accuracy varied between groups. It was good for groups *G*1 and *G*4-5 with a sensibility of 0.90 and 0.86 and a specificity of 0.97 and 0.98, respectively. More difficulties were observed to classify the subjects of *G*3 and especially those of *G*2.

The scatterplots showing the correlation between each of the network metrics and the cognitive score are presented in Figure 4. The cognitive score was positively correlated with the C_p, E_{loc}, and L_p values and negatively correlated with the E_g values. Hence, high level of performance at the neuropsychological tests was associated with more extended local clustering, higher ability of information to be propagated in the network, more efficient communication among neighbouring areas but less global efficiency of the network.

Functional Connectivity

The ANOVA revealed significant functional differences between groups (NBS corrected, $P < 0.01$) in the middle and inferior frontal gyri, the anterior cingular gyrus, the post central gyrus, the paracentral gyrus, the posterior insular area, the fusiform gyrus, the cuneus and superior

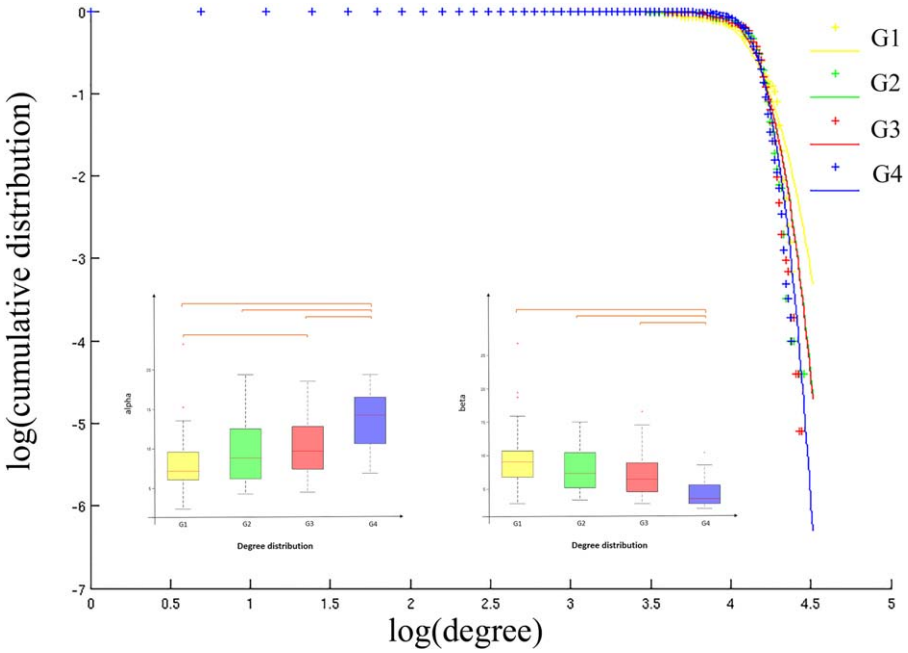

Figure 3.

Degree distribution. Plots of the log of the cumulative distribution of degree vs the log of degree, for each patients group. Cross points are the real data and lines are the estimated fitting. Boxplot of the distribution parameters and for each group. Between-group differences were assessed by one-way ANOVA and posthoc tests ($P < 0.01$). [Color figure can be viewed at wileyonlinelibrary.com]

occipital gyri, the calcarine sulcus, the striatum and the thalamus in the right hemisphere and in the inferior (opercular part) frontal and medial orbital frontal areas, the temporo-occipital areas, the striatum and the thalamus in the left hemisphere (Fig. 5 and Table IV). Further group comparisons are illustrated by the connectograms (Figs. 6 and 7) and revealed between-group differences in the architectural features of hub nodes and their connections (Table IV). Patients in *G*1 had higher hub connections of the right associative frontal and occipital areas than in *G*2. Compared with *G*3, *G*1 had also higher hub connections of the associative frontal, parietal, occipital areas, of the limbic cingular gyrus and temporal areas in the right hemisphere, as well as higher hub connections of a part of the associative temporal area in the left hemisphere. Compared with *G*4-5, *G*1 had higher hub connections of the associative frontal, temporal, occipital areas, the sensorimotor areas, the insular area, and the limbic cingular gyrus in the right hemisphere and of the insular sulcus, the associative temporal and occipital areas, the accumbens nucleus and hypothalamic area in the left hemisphere. Compared with *G*3, *G*2 had higher hub connections of the limbic and associative temporal areas in the right hemisphere and higher hub connections of the associative frontal sulcus and temporo-occipital areas in the left hemisphere. Compared with *G*4-5, *G*2 had higher hub connections of the associative frontal, parietal and temporal areas, of the limbic cingular and temporal areas, the primary visual area and the thalamus in the right hemisphere and higher hub connections of the associative temporal and occipital areas, of sensorimotor areas in the left hemisphere. Compared with *G*4-5, *G*3 had higher hub connections of the associative frontal areas, of the limbic frontal and cingular areas, limbic anterior cingular, the primary sensorimotor areas, the associative temporal and occipital areas in the right hemisphere and higher hub connections of the limbic frontal and cingular areas, in the left hemisphere.

TABLE III. Performance of subjects' classification based on graph-theory measures

	*G*1	*G*2	*G*3	*G*4-5
Sensitivity	0.90	0.48	0.79	0.86
Specificity	0.97	0.89	0.80	0.98

DISCUSSION

By classifying Parkinson's disease patients according to a spectrum of severity in cognitive impairment, we found a corresponding spectrum of changes in brain-network

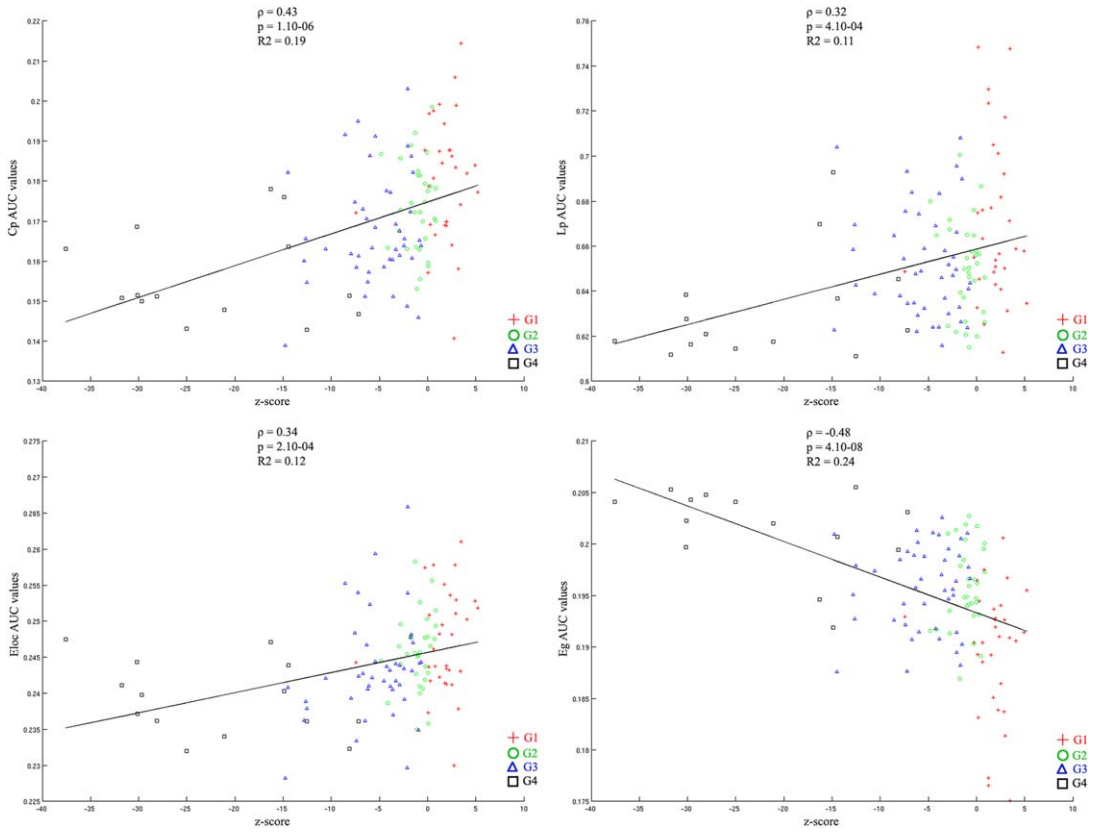

Figure 4.

Scatterplots showing the correlation between each of AUC network metrics values and performance at themost discriminant neuropsychological tests (composite cognitive score). AUC value corresponds to the area under the curve in plotting the network metric values as a function of the threshold values applied to the connectivity matrix. [Color figure can be viewed at wileyonlinelibrary.com]

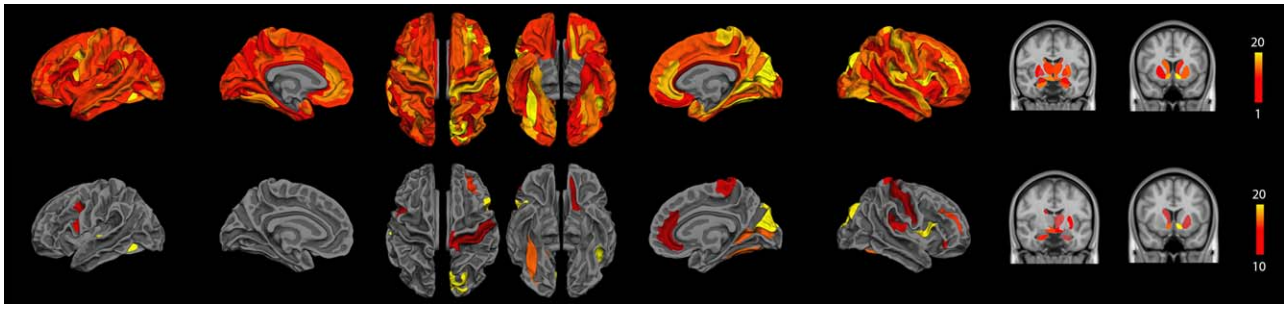

Figure 5.

Significant difference in terms of functional connections between groups as determined by one-way ANOVA (NBS corrected, $P < 0.01$). (top) Significant cortical nodes are projected onto the 74 cortical regions of interest segmented with Freesurfer and significant subcortical nodes were projected onto the MNI atlas. The colour code represents the number of significant connections of the given cortical ROI, from red representing one single connection and yellow more than 20. (bottom) Significant cortical and subcortical nodes with a number of significant connections higher than 10 are displayed. [Color figure can be viewed at wileyonlinelibrary.com]

TABLE IV. Localization of functional connectivity between-group differences

A. Significant group differences (ANOVA, $P < 0.01$ NBS-corrected for multiple comparisons). Only cortical and subcortical regions with a number of significant connections higher than 10 are reported.

			MNI coordinates		
Brain area	Side	**Specific area** (Freesurfer labels)	x	y	*z*
Frontal	Left	Orbital median sulcus (olfactory)	−12	25	−17
		Precentral sulcus-superior part	−23	−13	55
		Precentral sulcus-inferior part	−38	3	24
	Right	Middle frontal sulcus	28	47	13
		Frontal inferior gyrus - orbital	48	35	−9
		Frontal inferior gyrus - opercular	53	14	7
Parietal	Right	Postcentral gyrus	47	−27	58
		Central sulcus	20	−26	55
		Paracentral gyrus and sulcus	6	−31	61
Temporal	Left	Transverse temporal sulcus	−58	−28	7
		Lateral temporo-occipital sulcus	−41	−63	−11
		Hippocampus	−22	−18	18
	Right	Lateral occipito-temporal/fusiform gyrus	33	−53	−16
		Hippocampus	22	−18	18
Occipital	Right	Superior occipital gyrus	13	−86	28
		Calcarine sulcus	27	−65	4
		Cuneus gyrus	6	−78	18
Cingular	Right	Anterior cingular gyrus & sulcus	15	42	3
Insular	Right	Lateral fissure—posterior part	33	−29	16
Basal ganglia	Left	Accumbens nucleus	−9	9	−7
		Caudate nucleus	−9	12	5
		Thalamus	−10	−20	−11
	Right	Accumbens nucleus	9	9	−7
		Putamen	29	3	−1
		Thalamus	13	−14	9
			10	−20	−11

B. Group comparisons (two-sample t-test, $P < 0.01$ NBS-corrected for multiple comparisons)

			MNI coordinates		
Contrast	Side	**Brain area** (Freesurfer labels)	x	y	*z*
*G*1 vs. *G*2	Right	Superior frontal sulcus	22	30	35
		Superior occipital gyrus	13	−86	28
*G*1 vs. *G*3	Left	Transverse temporal sulcus	−58	−28	7
	Right	Superior frontal sulcus	22	30	35
		Middle frontal sulcus	28	47	13
		Cingular gyrus & sulcus (middle & posterior)	12	−10	48
		Superior temporal gyrus-planum polare	33	4	−25
		Superior parietal gyrus	30	−46	64
		Superior occipital gyrus	13	−86	28
		Inferior occipital gyrus and sulcus	34	−85	19
*G*1 vs. *G*4	Left	Anterior circular insular sulcus	−29	25	−3
		Transverse temporal sulcus	−58	−28	7
		Superior temporal sulcus	−56	−23	−5
		Posterior transverse collateral sulcus	−22	−56	19
		Accumbens	−9	9	−7
		Thalamus	−10	−20	−11
	Right	Inferior frontal gyrus (opercular)	42	10	5
		Precentral gyrus	35	−24	56
		Superior circular insula sulcus	40	10	8
		Cingular gyrus (posterior and ventral)	3	−50	15

TABLE IV. (continued).

B. Group comparisons (two-sample t-test, $P < 0.01$ NBS-corrected for multiple comparisons)

Contrast	Side	**Brain area** (Freesurfer labels)	MNI coordinates		
			x	y	z
		Temporal pole	41	18	−32
		Superior Temporal gyrus - Planum temporale	59	−29	8
		Post-central gyrus	45	−27	58
		Cuneus gyrus	6	−78	18
		Middle occipital gyrus	38	−89	−3
		Superior Occipital gyrus	−13	−86	28
*G*2 vs. *G*3	Left	Medial occipito-temporal/lingual gyrus	−18	−40	−13
		Inferior frontal sulcus	−40	32	14
	Right	Medial occipito-temporal/parahippocampal gyrus	29	−14	33
		Lateral occipito-temporal/fusiform gyrus	33	−53	−16
*G*2 vs. *G*4	Left	Superior lateral temporal gyrus	−67	−29	8
		Transverse temporal sulcus	−58	−28	7
		Superior temporal gyrus - planum temporale	−59	−29	8
		Paracentral gyrus and sulcus	−6	−31	61
		Post central sulcus	−47	−27	58
		Lateral occipital-temporal sulcus	−33	−53	−16
		Medial occipital-temporal (lingual gyrus)	−18	−40	−13
		Inferior occipital gyrus & sulcus	−34	−85	−19
		Middle occipital (lunatus sulcus)	−33	−89	−3
	Right	Inferior frontal gyrus (orbital)	48	35	−9
		Inferior frontal gyrus (opercular)	42	10	5
		Cingular gyrus & sulcus (middle anterior)	2	11	32
		Cingular gyrus & sulcus (middle posterior)	12	−10	48
		Temporal pole	41	18	−32
		Inferior parietal gyrus (angular)	46	−63	36
		Lateral occipito-temporal/fusiform gyrus	33	−53	−16
		Calcarine sulcus	−27	−65	4
		Thalamus	−13	−14	9
*G*3 vs. *G*4	Left	Orbital-H-shaped sulcus	−24	38	−15
		Medial orbital olfactory sulcus	−11	38	−22
		Anterior cingular gyrus & sulcus	−15	42	3
	Right	Orbital gyrus	16	30	−23
		Inferior Frontal gyrus (triangular)	47	26	14
		Superior Frontal gyrus	22	30	35
		Central sulcus	20	26	55
		Anterior cingular gyrus & sulcus	15	42	3
		Superior temporal gyrus - planum temporale	59	−29	8
		Post central gyrus	47	−27	58
		Anterior occipital sulcus	−47	−62	0

organization and connectivity at rest. More specifically, the local connectivity properties, i.e., functional network segregation (measured by the clustering coefficient and local efficiency, indices of local interconnectivity of a network), decreased as cognitive impairment worsened. Group differences in functional connectivity mainly concerned the ventral prefrontal, parietal, temporal and occipital cortices. The number of altered connections between the nodes of the network increased as cognitive impairment worsened. One of the key results of this study is that, even cognitively intact patients with only slight mental slowing (*G*2) already have reduced connectivity of two highly associative areas, the dorsolateral frontal cortex and the extrastriate cortex. This suggests that deficits in multimodal integration could be at the origin of very subtle cognitive impairment in Parkinson's disease, appearing early in the course of the disease. As cognitive impairment worsens (*G*3), reduced connectivity of the parietal and temporal regions is also observed in addition to the dorsolateral frontal cortex and the extrastriate cortex, in relation with the attention and executive functions impairment exhibited by that subgroup. In patients with severe cognitive impairment (*G*4-5), the pattern of connectivity is largely modified.

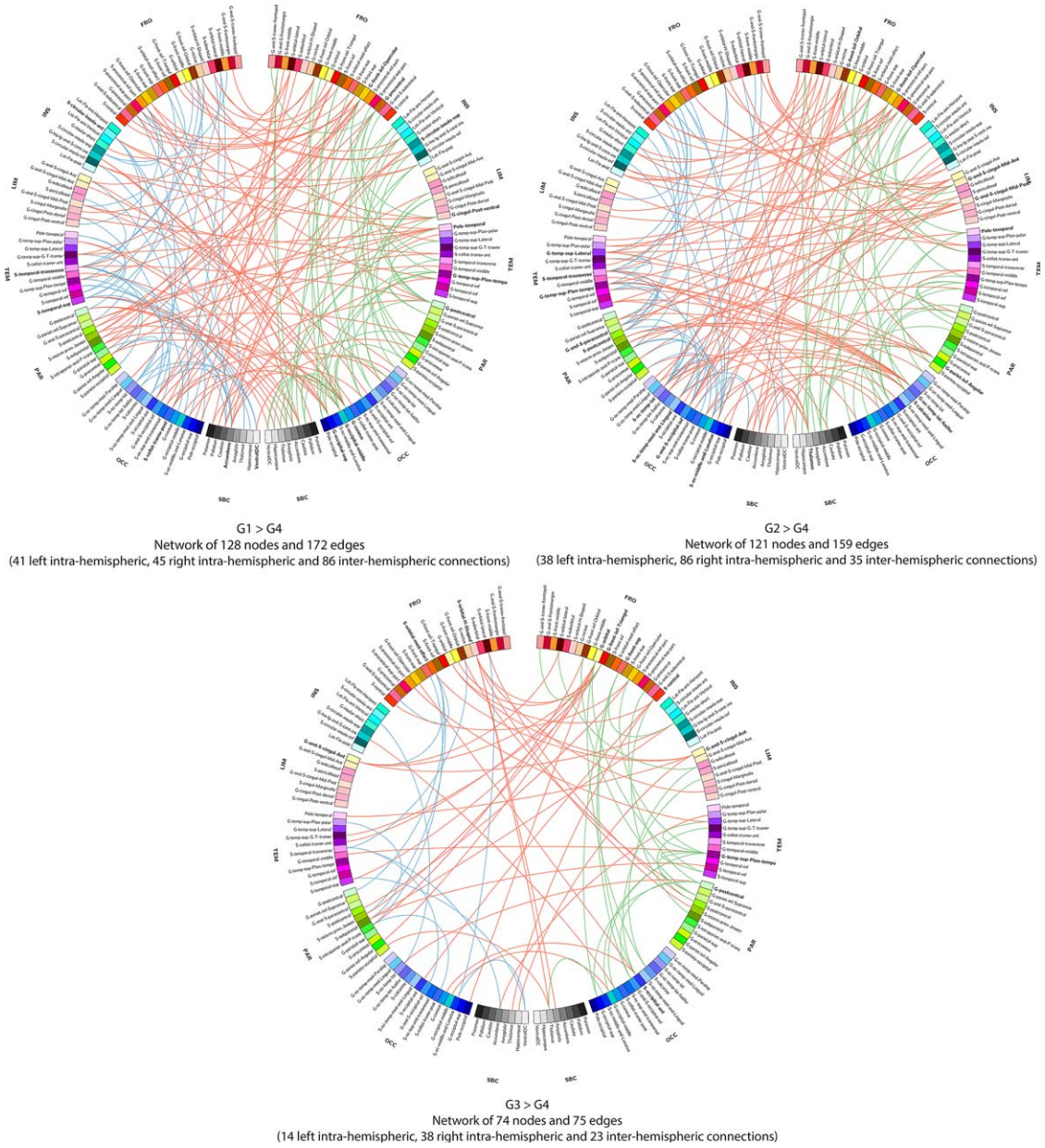

Figure 6.

Connectograms comparing patients from groups 1, 2, and 3 with patients from group 4 (NBS corrected, $P < 0.01$). Links are colored by connection type: left intra-hemispheric (blue), inter-hemispheric (red) and right intra-hemispheric (green). Regions of interests are grouped according to broad anatomical divisions [i.e., frontal (Fro), insular (Ins), cingular limbic (Lim), temporal (Tem), parietal (Par), occipital (Occ) or subcortical (Sbc)]. Bold regions represent "network hubs," which means regions with a high degree of significant connection. [Color figure can be viewed at wileyonlinelibrary.com]

Effects of Cognitive Impairment on Brain Network Topology

As shown by the progressive decrease of the values of clustering coefficient and local efficiency as cognitive impairment increased, there was a reduction of the functional segregation of the brain with cognitive impairment. According to Rubinov and Sporns, functional segregation is "the ability for specialized processing to occur within densely interconnected groups of brain regions" [Rubinov and Sporns, 2010]. This suggests that cognitive deficits in Parkinson's disease could be related to a

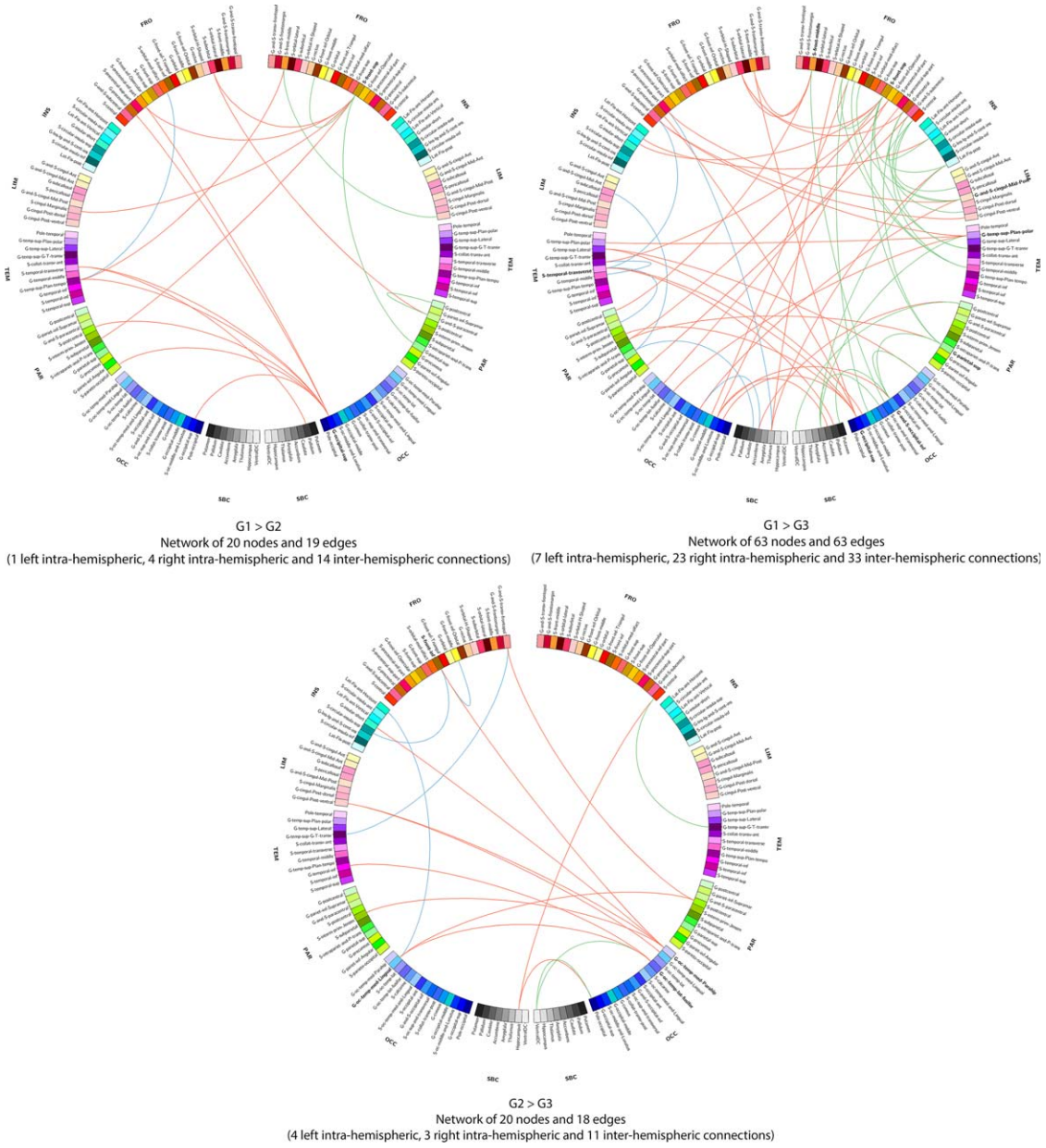

Figure 7.

Connectograms comparing patients from groups 1, 2 and 3 (NBS corrected, $P < 0.01$). Links are colored by connection type: left intra-hemispheric (blue), inter-hemispheric (red) and right intra-hemispheric (green). Regions of interests are grouped according to broad anatomical divisions [i.e., frontal (Fro), insular (Ins), cingular limbic (Lim), temporal (Tem), parietal (Par), occipital (Occ) or subcortical (Sbc)]. Bold regions represent "network hubs", which means regions with a high degree of significant connections. [Color figure can be viewed at wileyonlinelibrary.com]

progressive decrease in the density of connections between brain areas involved in specialized networks engaged in cognition. This is in line with the results of previous studies investigating functional connectivity of specific networks in Parkinson's disease. Hence, Tessitore et al. reported a decreased functional connectivity within the DMN in Parkinson's disease patients compared with healthy controls, which was correlated specifically with performance at cognitive tests but not with disease duration, motor impairment, or levodopa therapy [Tessitore et al., 2012]. In a 3-year follow-up of 36 Parkinson's disease patients and 12 healthy controls, Olde Dubbelink

et al. showed that functional connectivity decreased more in Parkinson's disease patients, especially in posterior parts of the brain and these changes were correlated with cognitive decline [Olde Dubbelink et al., 2014].

The increase of global efficiency and the trend toward a decrease in path length with higher cognitive impairment is more difficult to interpret. Indeed, these are measures of global network functioning, or functional network integration, and reflect "the ease with which brain regions communicate" [Rubinov and Sporns, 2010] and one may expect that these network metrics changed in the opposite direction when cognitive impairment increases. This apparently contradictory result could be explained as follows. Firstly, to check if it was an artefact or a result related to Parkinson's disease as a whole, we compared our results with that of a group of healthy subjects coming from another study but matched for sex, age and education with our participants (demographic details are shown in Supporting Information Table S1). Again, we found that global efficiency was lower and path length higher in that group than in the groups with cognitive impairment (Supporting Information Fig. S1). Moreover, there was no difference between this healthy control group and our cognitively intact group (*G*1) suggesting that the effects we observed on brain network measures were not related to Parkinson's disease, per se, but to cognitive impairment. The same pattern of results was observed for the degree distribution (Supporting Information Fig. S2). Secondly, this phenomenon could be interpreted in using all measures. Indeed, networks can be modelled within a framework of regular, random and complex networks. Regular networks have high local and low global connectivity, while random networks show the opposite pattern with low local and high global connectivity. The human brain network is inherently complex with an optimised balance between local and global connectivity, the so-called small-world network [Sporns, 2011]. Increased global efficiency together with decreased mean path length and less fat-tailed degree distribution indicate excessive network integration in cognitively impaired patient groups. These network features associated with decreased clustering coefficient and local efficiency are characteristic of a brain topology that shifts from a *small-world* towards a *random* network topology. Randomness increases with age and Smit et al. showed that the small-world pattern of adult age is gradually replaced by a more random topology at higher ages [Smit et al., 2010]. Moreover, it is also an indicator of network alterations in disease states [Stam, 2014]. Hence, the increase in global efficiency and the trend toward a decrease in path length we observed here with higher cognitive impairment may reflect an increase in randomness as cognitive impairment worsens in Parkinson's disease. Randomness of the brain network may thus be a marker of cognitive decline in Parkinson's disease. This is also confirmed by the pattern of correlations we observed between the network metrics and the composite cognitive score since more extended local clustering, higher ability of information to be propagated in the network, more efficient communication among neighboring areas but less global efficiency of the network were associated with higher level of performance at the neuropsychological tests.

When comparing PD-MCI and healthy controls, Baggio et al. reported a reduction of inter-network connections in PD-MCI, while local interconnectedness increased [Baggio et al., 2014; Baggio et al., 2015b]. This seems at odds with our own results. However, these studies used different approaches. Firstly, in our study, the groups of patients were not determined a priori but resulted from a cluster analysis identifying different levels of severity in cognitive impairment. Secondly, some differences in our methodology could explain our results with those of Baggio et al. (Baggio et al., 2014). Although the spatial normalization to MNI atlas is a common step in neuroimaging, their approach may cause inaccuracies of spatial transformation due to inter-subject anatomical variations that exist between the MNI template and the transformed data. To avoid this spatial normalization step, we worked in the individual subject space. Moreover, whereas the statistical analyses at the network level differed in both studies, we used AUC values calculated in a sparsity range of the connectivity matrix instead of testing each sparsity level.

Effects of Cognitive Impairment on Brain Functional Connectivity

The NBS analyses showed that alteration of brain network functional connectivity progressively increased, as cognitive impairment worsened. In Parkinson's disease patients with only slight mental slowing, weakened connections concerned the dorsolateral frontal cortex and the extrastriate cortex, two highly associative areas. Examination of the connectogram (Fig. 7 top-left) shows that these alterations mainly concerned interhemispheric connections to the frontal, temporal and parietal cortex. Changes in the fronto-parietal attentional network [Petersen and Posner, 2012] agree with the attention/executive functions deficits usually described in Parkinson's disease patients [Kehagia et al., 2013] but loss of connections from the extrastriate cortex to the temporal and parietal areas may be an early marker of cortical posterior dysfunction leading to deficits in memory and visuospatial functions [Kehagia et al., 2013] and increasing the risk of progression to dementia [Williams-Gray et al., 2007]. Such changes in brain functional connectivity may thus exist before performance at neuropsychological tests assessing these functions significantly declines. Markers of functional connectivity may thus be used in further cohort studies in order to determine whether they contribute to early identification of Parkinson's disease patients at risk of cognitive impairment or dementia.

When comparing cognitively intact patients with only slight mental slowing with patients with mild to moderate deficits, mainly in executive functions, weakened connections concerned interhemispheric connections from the posterior cortex to the parietal, temporal, cingular, insular and frontal regions (Fig. 7 bottom). Again, this suggests that an alteration of the functional connections from the posterior cortex may exist before deficits on tests usually assessing cortical posterior functions are observed. Moreover, this alteration seems to contribute to the dysexecutive syndrome through the long-range connections of the posterior cortex to the frontal, parietal and cingular cortex. Only a follow-up of these three groups of patients may determine the predictive value of these biomarkers.

When cognitive deficits are severe in all domains, the functional network was widely altered.

The changes in brain functional connectivity were analyzed and discussed here taking into account the spectrum of severity of cognitive decline we had previously observed. Further analyses are obviously needed to determine whether deficits in specific cognitive domains are associated with alterations within specific functional sub-networks.

Limitations

Several limitations of the current study should be considered. Firstly, due to our study design (data-driven approach in order to identify cognitive phenotypes in Parkinson's disease), we did not include a healthy control group and *G*1 (cognitively intact patients) was considered as our reference group. Hence, we were not able to identify changes in functional connectivity in this group compared with healthy controls. Nevertheless, our additional analysis on global network parameters (see Supporting Information) included a healthy control group and exhibited no difference between that group and *G*1, reinforcing the assumption that patients in *G*1 are cognitively intact, behave as healthy controls and can be considered as a reference group.

Secondly, due to the small number of subjects in the two groups with severe cognitive deficits, we decided to merge these two groups to perform the functional analyses although they were characterized by different cognitive profiles according to the cluster analysis. This has prevented any possibility of identifying connectivity differences between those groups. Moreover, despite the fact that the two groups with severe cognitive deficits were merged, the number of subjects of this category remains small. This is partly due to the exclusion of patients with moderate and severe dementia from the study in order to avoid missing data. By consequence, patients with severe cognitive deficits are underrepresented. Thirdly, patients were assessed after having received their usual antiparkinsonian medication ("best on" state) and dopaminergic medication may have influenced connectivity patterns. However, there were no group differences in terms of levodopa equivalent daily dose and it is unlikely that this factor may explain the observed differences. Finally, apathy and hallucinations were not considered as confounding factors in our analyses although previous studies showed alterations of resting-state functional connectivity in PD patients with apathy [Baggio et al., 2015a] or repetitive, complex visual hallucinations [Yao et al., 2014]. However, we considered that lack of initiative, reduction of interests and loss of insight may be symptoms of cognitive impairment since both apathy and hallucinations are embedded with cognitive impairment in Parkinson's disease. Adjusting these variables, in addition to reducing statistical power, would have removed useful information from our analyses.

Further Methodological Considerations

Several issues remain to be addressed. First, in this study, the regions of interest were obtained according to the parcellation of Fischl. Given the dependence of topological properties of brain networks and ROI definition [Wang et al., 2009], it would be interesting to use several parcellation systems to confirm the results. Nevertheless, this parcellation is well validated and no spatial normalization to MNI atlas is needed. Second, the head motion of subjects might have confounding effects on the final results of network analysis. To evaluate whether the results of network and edge analyses were affected by head motions, an autoregressive model AR(p) of order $P = 1$ was learned on the time series of the motions. The correlation between the AR(1) model coefficient of each time-course and network or edge measures was calculated by using a multivariate model [Salvador et al., 2008]. No significant correlations ($P > 0.05$) were found. Third, the brain network topology measures were calculated on binarized graphs that were constructed by thresholding the functional connectivity matrices. Although the use of binarized graphs reduced the complexity of network analysis, it also removed some detailed information. Further analyses could be conducted by using weighted correlation values ("weighted" graphs) instead of binarized graphs.

CONCLUSION

Our results revealed that progressive cognitive decline in Parkinson's disease is associated with changes in brain connectivity at rest. Topological organization of the network was progressively disrupted as cognitive impairment worsens, with increasing random organization of the network. Changes in functional connectivity between brain regions were observed even in patients with only slight mental slowing and mainly concerned highly associative areas. Although this needs confirmation in further cohort studies, the association of slowed mental processing speed with a lack in multimodal integration (revealed by brain connectivity analysis) could be an early marker of cognitive impairment in

Parkinson's disease and may contribute to the detection of prodromal forms of Parkinson's disease dementia.

REFERENCES

Aarsland D, Zaccai J, Brayne C (2005): A systematic review of prevalence studies of dementia in Parkinson's disease. Mov Disord 20:1255–1263.

Aarsland D, Taylor J-P, Weintraub D (2014): Psychiatric issues in cognitive impairment. Ed. David Burn, Daniel Weintraub, Trevor Robbins. Mov Disord 29:651–662.

Achard S, Salvador R, Whitcher B, Suckling J, Bullmore E (2006): A resilient, low-frequency, small-world human brain functional network with highly connected association cortical hubs. J Neurosci 26:63–72.

Andersson JLR, Skare S, Ashburner J (2003): How to correct susceptibility distortions in spin-echo echo-planar images: Application to diffusion tensor imaging. Neuroimage 20:870–888.

Baggio H-C, Sala-Llonch R, Segura B, Marti M-J, Valldeoriola F, Compta Y, Tolosa E, Junqué C (2014): Functional brain networks and cognitive deficits in Parkinson's disease. Hum Brain Mapp 35:4620–4634.

Baggio H-C, Segura B, Garrido-Millan JL, Marti M-J, Compta Y, Valldeoriola F, Tolosa E, Junqué C (2015a): Resting-state frontostriatal functional connectivity in Parkinson's disease-related apathy. Mov Disord 30:671–679.

Baggio H-C, Segura B, Sala-Llonch R, Marti M-J, Valldeoriola F, Compta Y, Tolosa E, Junqué C (2015b): Cognitive impairment and resting-state network connectivity in Parkinson's disease. Hum Brain Mapp 36:199–212.

Baker STE, Lubman DI, Yücel M, Allen NB, Whittle S, Fulcher BD, Zalesky A, Fornito A (2015): Developmental changes in brain network hub connectivity in late adolescence. J Neurosci 35:9078–9087.

Barone P, Aarsland D, Burn D, Emre M, Kulisevsky J, Weintraub D (2011): Cognitive impairment in nondemented Parkinson's disease. Mov Disord 26:2483–2495.

Behzadi Y, Restom K, Liau J, Liu TT (2007): A component based noise correction method (CompCor) for BOLD and perfusion based fMRI. Neuroimage 37:90–101.

Benton AL, Varney NR, Hamsher KD (1978): Visuospatial judgment. A clinical test. Arch Neurol 35:364–367.

Biswal B, Yetkin FZ, Haughton VM, Hyde JS (1995): Functional connectivity in the motor cortex of resting human brain using echo-planar MRI. Magn Reson Med 34:537–541.

Brandt J, Benedict R (2001): Hopkins Verbal Learning Test-Revised. Lutz, FL: Psychological Assessment Resources.

Bressler SL, Menon V (2010): Large-scale brain networks in cognition: Emerging methods and principles. Trend Cogn Sci (Regul Ed) 14:277–290.

Bullmore E, Sporns O (2009): Complex brain networks: graph theoretical analysis of structural and functional systems. Nat Rev Neurosci 10:186–198.

Buter TC, van den Hout A, Matthews FE, Larsen JP, Brayne C, Aarsland D (2008): Dementia and survival in Parkinson disease: A 12-year population study. Neurology 70:1017–1022.

Dale AM, Fischl B, Sereno MI (1999): Cortical surface-based analysis. I. Segmentation and surface reconstruction. Neuroimage 9:179–194.

de Lau LML, Breteler MMB (2006): Epidemiology of Parkinson's disease. Lancet Neurol 5:525–535.

Dujardin K, Sockeel P, Delliaux M, Destée A, Defebvre L (2009): Apathy may herald cognitive decline and dementia in Parkinson's disease. Mov Disord 24:2391–2397.

Dujardin K, Leentjens AFG, Langlois C, Moonen AJH, Duits AA, Carette A-S, Duhamel A (2013): The spectrum of cognitive disorders in Parkinson's disease: A data-driven approach. Mov Disord 28:183–189.

Dujardin K, Moonen AJH, Behal H, Defebvre L, Duhamel A, Duits AA, Plomhause L, Tard C, Leentjens AFG (2015): Cognitive disorders in Parkinson's disease: Confirmation of a spectrum of severity. Parkinsonism Relat Disord 21:1299–1305.

Elgh E, Domellöf M, Linder J, Edström M, Stenlund H, Forsgren L (2009): Cognitive function in early Parkinson's disease: A population-based study. Eur J Neurol 16:1278–1284.

Emre M (2003): Dementia associated with Parkinson's disease. Lancet Neurol 2:229–237.

Emre M, Aarsland D, Brown R, Burn DJ, Duyckaerts C, Mizuno Y, Broe GA, Cummings J, Dickson DW, Gauthier S, Goldman J, Goetz C, Korczyn A, Lees A, Levy R, Litvan I, McKeith I, Olanow W, Poewe W, Quinn N, Sampaio C, Tolosa E, Dubois B (2007): Clinical diagnostic criteria for dementia associated with Parkinson's disease. Mov Disord 22:1689. 707– quiz 1837.

Fox MD, Raichle ME (2007): Spontaneous fluctuations in brain activity observed with functional magnetic resonance imaging. Nat Rev Neurosci 8:700–711.

Gibb WR, Lees AJ (1988): The relevance of the Lewy body to the pathogenesis of idiopathic Parkinson's disease. J Neurol Neurosurg Psychiatr 51:745–752.

Goetz CG, Tilley BC, Shaftman SR, Stebbins GT, Fahn S, Martinez-Martin P, Poewe W, Sampaio C, Stern MB, Dodel R, Dubois B, Holloway R, Jankovic J, Kulisevsky J, Lang AE, Lees A, Leurgans S, LeWitt PA, Nyenhuis D, Olanow CW, Rascol O, Schrag A, Teresi JA, van Hilten JJ, LaPelle N; Movement Disorder Society UPDRS Revision Task Force (2008): Movement Disorder Society-sponsored revision of the Unified Parkinson's Disease Rating Scale (MDS-UPDRS): Scale presentation and clinimetric testing results. Mov Disord 23:2129–2170.

Graves RE, Bezeau SC, Fogarty J, Blair R (2004): Boston naming test short forms: A comparison of previous forms with new item response theory based forms. J Clin Exp Neuropsychol 26:891–902.

Greve DN, Fischl B (2009): Accurate and robust brain image alignment using boundary-based registration. Neuroimage 48:63–72.

Halliday GM, McCann H (2010): The progression of pathology in Parkinson's disease. Ann N Y Acad Sci 1184:188–195.

Hamilton M (1960): A rating scale for depression. J Neurol Neurosurg Psychiatr 23:56–62.

Helmich RC, Derikx LC, Bakker M, Scheeringa R, Bloem BR, Toni I (2010): Spatial remapping of cortico-striatal connectivity in Parkinson's disease. Cereb Cortex 20:1175–1186.

Hoehn MM, Yahr MD (1967): Parkinsonism: onset, progression, and mortality. Neurology 57.

Holland D, Kuperman JM, Dale AM (2010): Efficient correction of inhomogeneous static magnetic field-induced distortion in Echo Planar Imaging. Neuroimage 50:175–183.

Hughes TA, Ross HF, Musa S, Bhattacherjee S, Nathan RN, Mindham RH, Spokes EG (2000): A 10-year study of the incidence of and factors predicting dementia in Parkinson's disease. Neurology 54:1596–1602.

Irimia A, Chambers MC, Torgerson CM, Van Horn JD (2012): Circular representation of human cortical networks for subject and population-level connectomic visualization. Neuroimage 60:1340–1351.

Kehagia AA, Barker RA, Robbins TW (2013): Cognitive impairment in Parkinson's disease: The dual syndrome hypothesis. Neurodegener Dis 11:79–92.

Leentjens AFG, Dujardin K, Pontone GM, Starkstein SE, Weintraub D, Martinez-Martin P (2014): The Parkinson anxiety scale (PAS): Development and validation of a new anxiety scale. Mov Disord 29:1035–1043.

Litvan I, Aarsland D, Adler CH, Goldman JG, Kulisevsky J, Mollenhauer B, Rodriguez-Oroz MC, Tröster AI, Weintraub D (2011): MDS task force on mild cognitive impairment in Parkinson's disease: Critical review of PD-MCI. Mov Disord 26: 1814–1824.

Morris JC (1993): The clinical dementia rating (CDR): Current version and scoring rules. Neurology 43:2412–2414.

Muslimovic D, Post B, Speelman JD, Schmand B (2005): Cognitive profile of patients with newly diagnosed Parkinson disease. Neurology 65:1239–1245.

Olde Dubbelink KTE, Schoonheim MM, Deijen JB, Twisk JWR, Barkhof F, Berendse HW (2014): Functional connectivity and cognitive decline over 3 years in Parkinson disease. Neurology 83:2046–2053.

Onnela J-P, Saramäki J, Kertész J, Kaski K (2005): Intensity and coherence of motifs in weighted complex networks. Phys Rev E Stat Nonlin Soft Matter Phys 71:065103.

Petersen SE, Posner MI (2012): The attention system of the human brain: 20 years after. Annu Rev Neurosci 35:73–89.

Power JD, Barnes KA, Snyder AZ, Schlaggar BL, Petersen SE (2012): Spurious but systematic correlations in functional connectivity MRI networks arise from subject motion. Neuroimage 59:2142–2154.

Prodoehl J, Burciu RG, Vaillancourt DE (2014): Resting state functional magnetic resonance imaging in Parkinson's disease. Curr Neurol Neurosci Rep 14:448.

Reid WGJ, Hely MA, Morris JGL, Loy C, Halliday GM (2011): Dementia in Parkinson's disease: A 20-year neuropsychological study (Sydney Multicentre Study). J Neurol Neurosurg Psychiatr 82:1033–1037.

Reitan RM (1992): TMT, Trail Making Test A & B. South Tucson.

Rektorova I, Krajcovicova L, Marecek R, Mikl M (2012): Default mode network and extrastriate visual resting state network in patients with Parkinson's disease dementia. Neurodegener Dis 10:232–237.

Rubinov M, Sporns O (2010): Complex network measures of brain connectivity: Uses and interpretations. Neuroimage 52: 1059–1069.

Salvador R, Martínez A, Pomarol-Clotet E, Gomar J, Vila F, Sarró S, Capdevila A, Bullmore E (2008): A simple view of the brain through a frequency-specific functional connectivity measure. Neuroimage 39:279–289.

Smit DJA, Boersma M, van Beijsterveldt CEM, Posthuma D, Boomsma DI, Stam CJ, de Geus EJC (2010): Endophenotypes in a dynamically connected brain. Behav Genet 40:167–177.

Smith A (1982): Symbol Digits Modalities Test. Los Angeles: Western Psychological Services.

Sockeel P, Dujardin K, Devos D, Deneve C, Destée A, Defebvre L (2006): The Lille apathy rating scale (LARS), a new instrument for detecting and quantifying apathy: Validation in Parkinson's disease. J Neurol Neurosurg Psychiatr 77:579–584.

Sporns O (2011): The human connectome: A complex network. Ann N Y Acad Sci 1224:109–125.

Stam CJ (2014): Modern network science of neurological disorders. Nat Rev Neurosci 15:683–695.

Tessitore A, Esposito F, Vitale C, Santangelo G, Amboni M, Russo A, Corbo D, Cirillo G, Barone P, Tedeschi G (2012): Default-mode network connectivity in cognitively unimpaired patients with Parkinson disease. Neurology 79:2226–2232.

Tomlinson CL, Stowe R, Patel S, Rick C, Gray R, Clarke CE (2010): Systematic review of levodopa dose equivalency reporting in Parkinson's disease. Mov Disord 25:2649–2653.

Tröster AI (2011): A Précis of recent advances in the neuropsychology of mild cognitive impairment(s) in Parkinson's disease and a proposal of preliminary research criteria. J Int Neuropsychol Soc 17:1–14.

Wang J, Wang L, Zang Y, Yang H, Tang H, Gong Q, Chen Z, Zhu C, He Y (2009): Parcellation-dependent small-world brain functional networks: A resting-state fMRI study. Hum Brain Mapp 30:1511–1523.

Watts DJ, Strogatz SH (1998): Collective dynamics of "small-world" networks. Nature 393:440–442.

Wechsler D (1986): WAIS-R: Wechsler adult intelligence scale, revised.

Williams-Gray CH, Foltynie T, Brayne CEG, Robbins TW, Barker RA (2007): Evolution of cognitive dysfunction in an incident Parkinson's disease cohort. Brain 130:1787–1798.

Wu T, Wang L, Chen Y, Zhao C, Li K, Chan P (2009): Changes of functional connectivity of the motor network in the resting state in Parkinson's disease. Neurosci Lett 460:6–10.

Wu T, Long X, Wang L, Hallett M, Zang Y, Li K, Chan P (2011): Functional connectivity of cortical motor areas in the resting state in Parkinson's disease. Hum Brain Mapp 32:1443–1457.

Yao N, Shek-Kwan Chang R, Cheung C, Pang S, Lau KK, Suckling J, Rowe JB, Yu K, Ka-Fung Mak H, Chua S-E, Ho S-L, McAlonan GM (2014): The default mode network is disrupted in Parkinson's disease with visual hallucinations. Hum Brain Mapp 35:5658–5666.

Zalesky A, Fornito A, Bullmore ET (2010): Network-based statistic: Identifying differences in brain networks. Neuroimage 53: 1197–1207.

Zalesky A, Cocchi L, Fornito A, Murray MM, Bullmore E (2012): Connectivity differences in brain networks. Neuroimage 60: 1055–1062.